A first trial for the new electrostatic generator that will solve the CO₂ problem

Katsuo Sakai

Electrostatic generator Laboratory

Yokohama Japan

phone: (81) 45-973-4014

e-mail: gy7a-ski@asahi-net.or.jp

Abstract—**For a long time, Electrostatics generator has been driven by a mechanical force. On the contrary, a new electrostatic generator was proposed recently. It is driven by Asymmetric electrostatic force in place of a mechanical force. Usually, magnitude of an electrostatic force that acts on an charged sphere conductor does not change when the direction of electric field is reversed. But, if the shape of the conductor is asymmetric, the magnitude changes remarkably. This interesting phenomenon was named as asymmetric electrostatic force. The new electrostatic generator uses an asymmetric conductor as a charge carrier.**

This time, a simple instrument of the new electrostatic generator was made. And, Its performance was measured. Unfortunately, this trial instrument failed to generate an electricity. The main reason of the failure is that the air resistance to the charge carrier was stronger than the electrostatic force. However this problem will be solved with a vacuum type instrument, and the new electrostatic generator will solve the CO₂ problem in the near future.

I. INTRODUCTION

A. Asymmetric electrostatic force

For a long time, the main purposes of electrostatic research have been electrophotography and electrospray coating. Both technologies make use of fine charged powders, which are moved by electrostatic force. The magnitude of the electrostatic force has been calculated by the well-known Coulomb's formula (1). It is apparent from this formula that the magnitude of this electrostatic force doesn't change when the direction of the electric field turns over as shown in figure 1.

$$f = qE \qquad (1)$$

where f: Electrostatic force that acts on the fine charged powder.
Q: Quantity of charge on the fine powder.
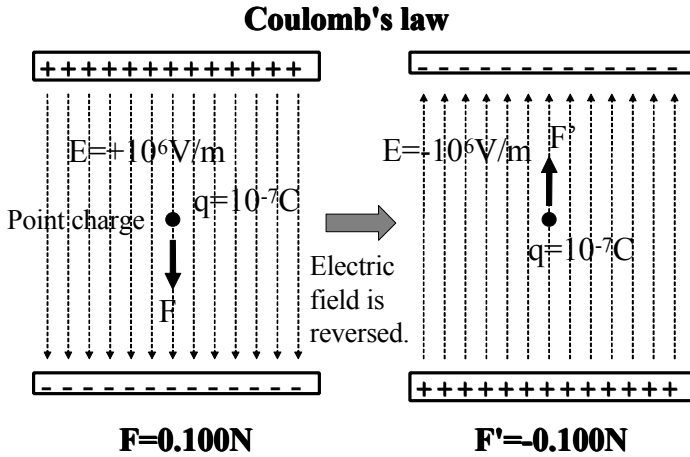E: Intensity of the electric field in which the fine powder is placed.

Coulomb's law

$E=+10^6V/m$ $E=-10^6V/m$ F'

Point charge $q=10^{-7}C$ Electric field is reversed. $q=10^{-7}C$

F

F=0.100N **F'=-0.100N**

Fig. 1. Electrostatic force that acts on a point charge (Coulom's law)

The application of this formula is limited to point charges and sphere-shaped charge carriers [1]. The charge on a fine powder has commonly been treated as a point charge.

In contrast, a new electrostatic generator that uses a non-spherical charge carrier was presented recently [2], [3], [4], [5]. This generator uses an asymmetric shape conductor as its charge carrier. The electrostatic force that acts on this asymmetric shape charge carrier was both simulated and experimentally measured [4], [5], [6], [7]. As a result, it has become clear that the magnitude of this electrostatic force reduces when the direction of the electric field is reversed as shown in figure 2.

Asymmetric electrostatic force

$E=+10^6V/m$ $q=10^{-7}C$ F'

Asymmetric charged conductor Electric field is reversed. $q=10^{-7}C$
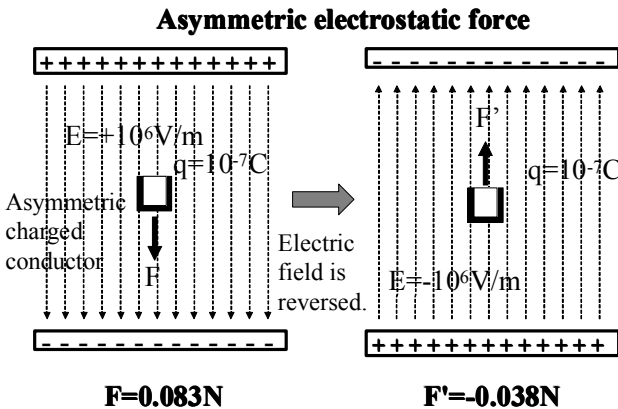
F $E=-10^6V/m$

F=0.083N **F'=-0.038N**

Fig. 2. Electrostatic force that acts on charged box conductor (Asymmetric electrostatic force).

And this changeable electrostatic force was named as Asymmetric electrostatic force unofficially.

B. Basic theory of the new electrostatic generator

The idea behind an electrostatic generator has been defined by lifting the charge to a high potential by mechanical force against the electric force that acts on this charge. It is impossible for the mechanical force to carry the charge directly. Therefore, the charge is packed into a suitable body. We call this body the charge carrier.

The most popular electrostatic generator is the Van de Graaff type electrostatic generator [8]. This was invented by Dr. Van de Graaff in 1931 in the USA. Today, it is used with a large voltage power supply. It can produce ten million volts. In this machine, an insulating belt is used as a charge carrier. Figure 3 shows an example of this generator.
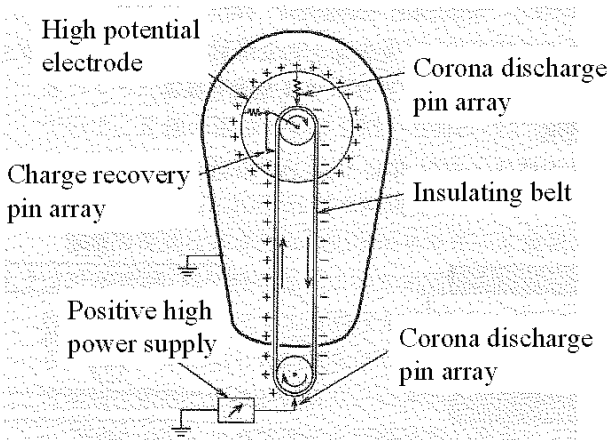

Fig. 3. Schematic layout of the Van de Graaff electrostatic generator .

The insulating belt is moved in the direction of the arrow by a motor. The bottom corona diskharge pin array places positive ions on the insulating belt. The positive ions on the insulating belt are carried to the high voltage electrode sphere by the mechanical force of a motor. Corona diskharge occurs between the negative charge on the recovery pin array and the positive ions on the insulating belt. As a result, the positive ions on the insulating belt are neutralized by the negative corona ions. Then, positive charges (holes) are added to the high voltage electrode sphere.

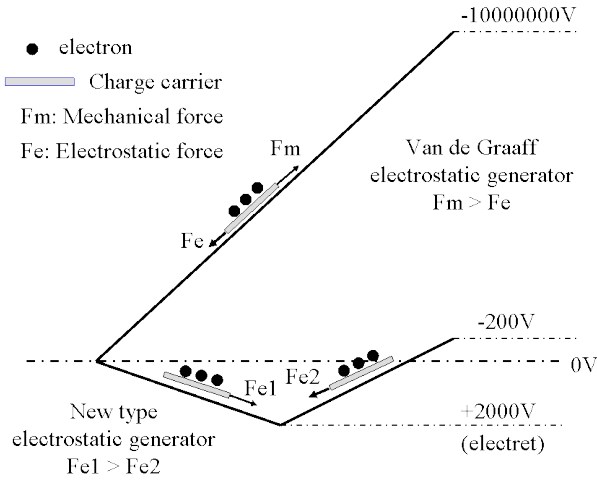The principle of this electrostatic generator is shown schematically in Fig. 4.

Fig. 4. Schematic explanation of the principles behind the two electrostatic generators.

In figure 4, the bold line represents the potential, and the arrows represent the forces. The small black circles represent the electrons, and the gray plates represent the charge carriers. In the Van de Graaff electrostatic generator, the charge carrier is directly transported by a strong mechanical force, Fm, against the electrostatic force Fe.

In contrast, in the new electrostatic generator, the charge carrier is firstly moved in the forward electric field caused by electrets according to the electrostatic force Fe1. In this process, the charge carrier gains kinetic energy from the electric field. Then, the carrier is moved in the backward electric field, expending the given energy against electrostatic force Fe2.

The shape of this charge carrier is asymmetric. Therefore, the asymmetric electrostatic force acts on this charge carrier. Thus, the absolute value of Fe1 is larger than that of Fe2. As a result, the charge carrier can arrive at a potential that is higher (-200 V) than the initial potential (0 V).

The new electrostatic generator cannot produce ten million volts, but it does not require mechanical force. It will be driven by the asymmetric electrostatic force that originates from the electric field of an electret. The electric field energy of the electret is infinite [9]. Therefore, if the lifetime of the electret is one hundred years, the new electrostatic generator could generate electric energy one hundred years without adding energy. As a result, this new electrostatic generator can solve the CO_2 problem.

C. Simulation results of the energy gained using the new electrostatic generator.

Now that the basic principle of the new electrostatic generator is clear, then, the electric energy gained by the smallest unit of the new generator is simulated. The smallest unit is concretely shown in figure 5 .
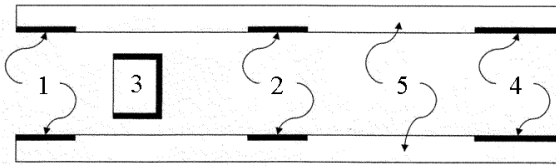
Fig. 5. Schematic layout of one unit of the new electrostatic generator.

This generator mainly consists of electrets 2, injection electrodes 1, and recovery electrodes 4. All of them are disposed on insulating base board 5. The distance between the boards is 0.240 mm. The width of the injection electrodes, the electrets, and the recovery electrodes is 0.080 mm, 0.120 mm, and 0.160mm respectively. The electrets, the injection electrodes, and the recovery electrodes have the same length of 38.000 mm. The distance between the electrets and the injection electrodes is 0.320 mm, and the distance between the electrets and the recovery electrodes is 0.320 mm as well.

The electrets have a semi-permanent positive charge density of +0.1 mC/m2. The injection electrodes are grounded. The recovery electrodes are kept at a voltage of -260 V. As a result, the electric potential of the electrets is approximately +2600 V.   Therefore, the electrets and the injection electrodes produce a forward electric field for a negative charge between them. The electrets and the recovery electrodes produce a backward electric field for a negative charge between them.

The long open box 3 is used for a charge carrier that carries negative charge (electron) from the injection electrodes to the recovery electrodes through the electrets. The height of the long box is 0.160 mm, and the width of the long box is 0.080 mm. The thickness of the wall of the long box is 0.02 mm. The length of the long box is 38.000 mm.

Figure 6 shows the left half of the cell design (mesh) for the simulation of one unit of the new electrostatic generator. The two dimension finite difference method [10], [11], [12] was used to simulate the electrostatic force that acts on the box shape charge carrier.
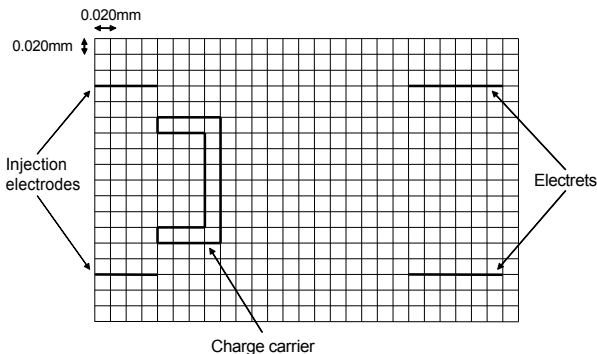

Fig. 6. A design of cells (mesh) to simulate the electrostatic force that acts on a charge carrier in one unit of the new electrostatic generator.

At first, the quantity of injection charge to the charge carrier from the injection electrode was simulated. The resulting charge was 0.586 nC. Electrostatic forces that acts on this charge carrier was simulated at an interval of 0.020 mm. The recovery electrodes were grounded in this simulation for simplicity. Figure 7 shows the results of the simulation.
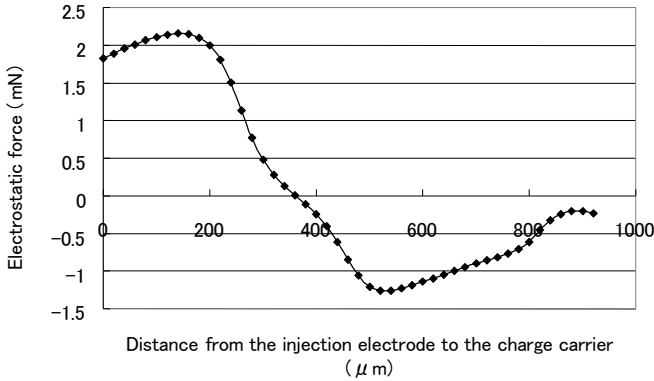

Fig. 7. Electrostatic force as a function of the distance from the injection electrode to the charge carrier.

The electrostatic force in the forward field (0-380 μ m) is positive; therefore, the charge carrier gains kinetic energy. In contrast, that becomes negative in the backward electric field (380-920 μ m). Then, the charge carrier loses some of its kinetic energy. As a result, the charge carrier maintains extra kinetic energy, 1.53E-7 J, when it arrives between the recovery electrodes. The carried charge quantity is -5.86E-10 C. This charge can be lifted to a higher potential by the extra energy. This possible potential is calculated to -261 V.

The carried charge cannot be recovered perfectly, because the recovery electrodes do not comprise a perfect Faraday gauge. The remaining charge on the charge carrier can be simulated by grounding the charge carrier between the recovery electrodes. The simulated remaining charge was -0.61E-10 C. As a result, the recovered charge was -5.25E-10 C, and the recovery rate was 90%.

In this one process, a charge of -5.25E-10 C was lifted to -261 V from 0 V. Therefore the generated electric energy was calculated to 1.37E-7 J. This is a small amount of energy, but a large amount of energy can be obtained by gathering those small units. The concrete design of the new electrostatic generator that can generate a large amount of energy is explained in the following chapter.

D. Manufacturing method of a new electrostatic generator

Fig. 8 shows an ideal structure of the electrode that is used as the charge carrier.
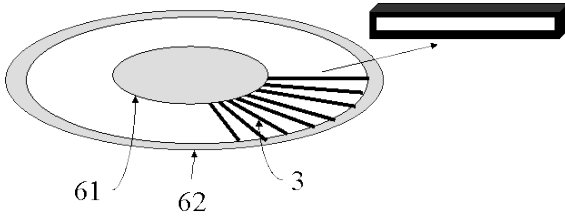
Fig. 8. Ideal structure of the box-type electrodes to be used as charge carriers.

In this ideal charge carrier disk, many long box electrodes 3 are oriented radially to the circumference 62 from the core 61 of the insulating base disk. This charge carrier disk is sandwiched between two electrode disks. Figure 9 shows one set of three disks of the new electrostatic generator.
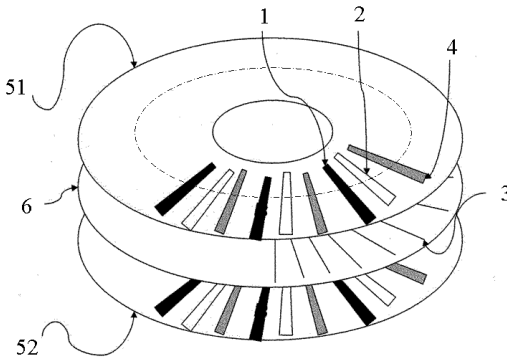

Fig. 9. Schematic layout of the one set of three disks of the new electrostatic generator.

In Fig. 9, mark 6 shows the charge carrier disk. Marks 51 and 52 show the upper electrode disk and the lower electrode disk, respectively. Mark 3 shows the charge carrier electrode. Marks 1, 2, and 4 show the injection electrode, the electrets, and the recovery electrode, respectively. These electrodes and electrets are made on one side of the electrode disk. The lower electrode disk has the same structure as the upper electrode disk. However, the electrode surfaces of the two electrode disks face each other. These two electrode disks are fixed, and the charge carrier disk rotates at a high speed.

When it rotates by 1000rpm, as a result the electric power generated by one set of three disks of the new electrostatic generator shown in figure 9 becomes to 0.236W. Therefore, the total electric power that a 1-m^3 box of the new electrostatic generator can generate becomes 32.125 kW.

The charge density of the electret used in the simulation is 0.1 mC/m^2. The maximum charge density of the electret that we can use today is 1.0 mC/m^2 [13]. As a result, the generated electric power becomes 3212.5 kW/m^3 .

In the above-described calculation, it was assumed that the air resistance that arises with the high rotational speed of the charge carrier disk is zero. This assumption can be made valid by making the inside of the set a vacuum. A vacuum has three other advantages as

well. One of them is that the corona diskharge never occurs. The second is that the charge on the charge carrier will never leak into the air moisture. If either of these occurs, the electret charge will be quickly neutralized. The third advantage is that oxidation of the surface of the charge carrier never occurs. If this occurs, the electrostatic force does not act on the surface of the charge carrier perpendicularly. As a result, the asymmetric electrostatic force decreases.

II. TRIAL INSTRUMENT OF THE NEW ELECTROSTATIC GENERATOR

The disk type new electrostatic generator that is shown in figure 9 is ideal. However, it is very difficult to make it by hand. Therefore, a switch-back structure is selected in place of the disk type. Accordingly, a cylinder-disk type charge carrier is selected in place of the box type charge carrier.

Figure 10 shows the front and side views of the cylinder-disk type charge carrier used in this experiment.
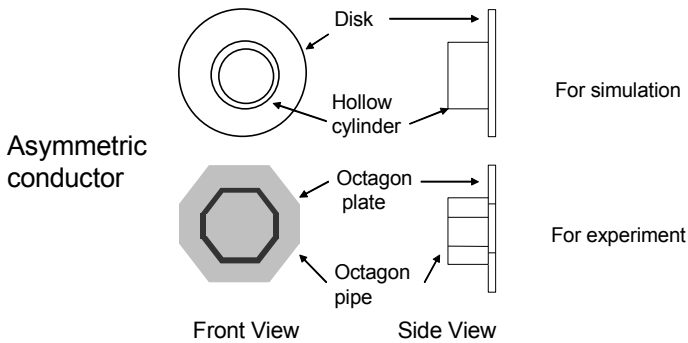

Fig. 10. The front and side view of the asymmetric charge carrier (for simulation and for experiment).

They are axis symmetrical shaped conductors. Because the latter mentioned simulation method can only simulate axis-symmetrical shaped conductors.

The asymmetric conductor consists of a disk and a hollow cylinder, as shown in figure 10. But, it actually consists of a octagon plate and a octagon pipe as shown in figure 10. Because it is very difficult to make a disk and a cylinder correctly by hand.

The diameters of the disk (octagon plate) and cylinder (octagon pipe) are 30.0 mm and 20.0 mm, respectively. The width of the cylinder (octagon pipe) is 10.0 mm. They were made from thin gilding aluminium plates. As a result, the electrostatic force always acts on the gold surface perpendicularly. The thicknesses of the disk (octagon plate) and cylinder (octagon pipe) is 0.1 mm. There are thirteen small apertures on the octagon plate. The air resistance to this surface might be reduced by those small apertures.

Because the asymmetric conductor was made by hand, the cylinder (octagon pipe) surface of the asymmetric conductor is not perfectly parallel to the direction of the electric field and the disk (octagon plate) surface is not perfectly perpendicular to the direction of the electric field.

Figure 11 shows the front view of the trial experiment instrument of the new electrostatic generator.
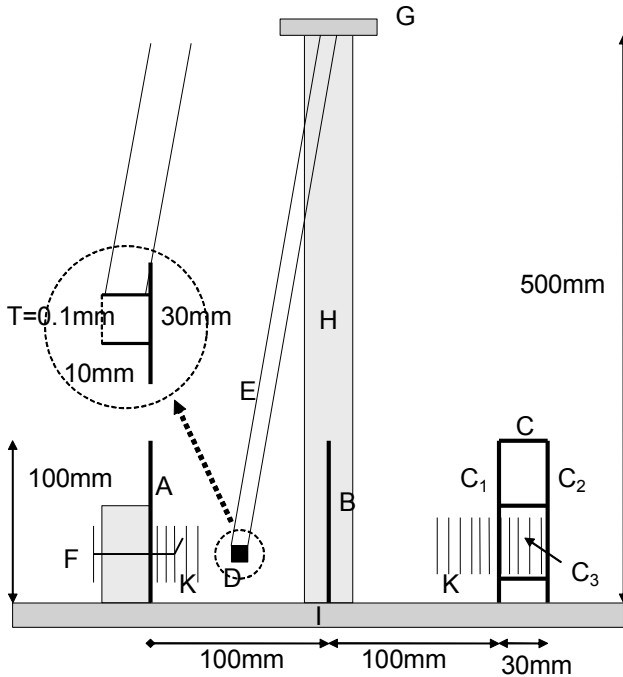
Fig. 11. The front view of the trial experiment instrument of the new electrostatic generator

In the figure 11, sign A shows a charge injection electrode that was grounded,
Sign B shows an high voltage electrode that was applied to high voltage,
(This electrode is replaced with electret when an actual electrostatic generator is made.)
Sign C shows a charge recovery electrode that was connected to capacitor,
Sign C_1 shows the front surface of the charge recovery electrode,
Sign C_2 shows the back surface of the charge recovery electrode,
Sign C_3 shows the side window of the charge recovery electrode for measuring an
    arrival position of the charge carrier using the scale K,
Sign D shows a octagon plate and pipe charge carrier that was electrically floated,
Sign E shows insulating threads that floated the charge carrier,
Sign F shows catapult that release the charge carrier,
Sign G shows insulating plate that held the threads,
Sign H shows insulating high pillar that held the plate,
Sign I shows insulating base plate,
Sign J shows a capacitor (See fig.14),
Sign K shows a scale for measuring positions of the charge carrier

In figure 11, the inside of big circle on the left is an enlarged picture of the charge carrier
(D). The three electrodes (A, B, C) were made from aluminium plate with 0.2mm
thickness and the charge carrier (D) was made from gilding aluminium plate with 0.1mm

thickness. The insulating thread (E) was made from raw silk that is used by Japanese kimono. The other insulating parts (F, G, H, I) consisted of Acryl or Polypropylene resin.

Figure 12 shows the side view of the center of the trial experiment instrument.
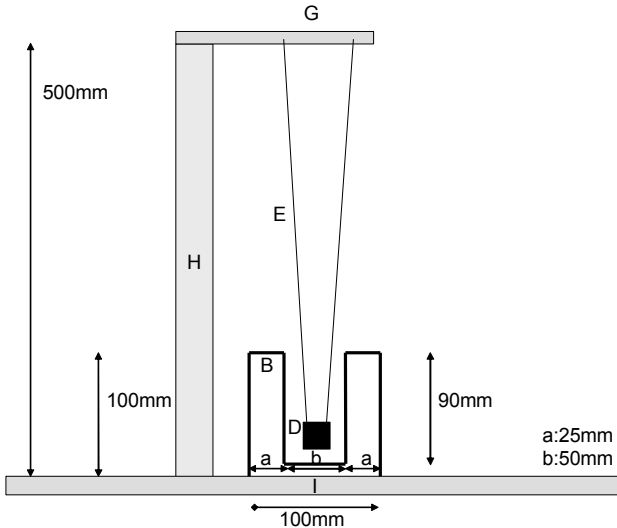

Fig. 12. The side view of the center of the trial experiment instrument of the new electrostatic generator

The high voltage electrode (B) was partly cut out as shown in figure 12 at the center. As a result, the charge carrier (D) can pass through the high voltage electrode (B). The distance between the charge carrier (D) and the edge of the cut part of the high voltage electrode (B) was 10mm. And the edge of the cut part was covered with TEFLON tape. As a result, Corona diskharge between the edge and the charge carrier (D) was prevented.

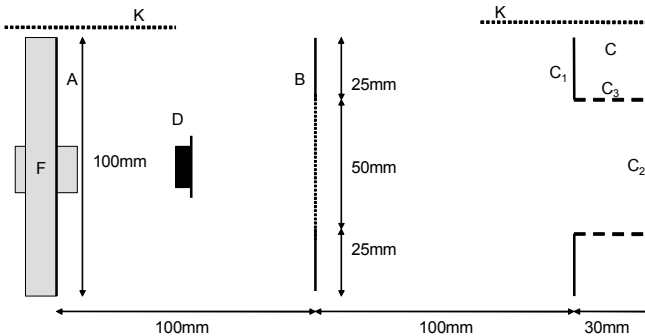Figure 13 shows the plane view of the trial experiment instrument.

Fig. 13. The plane view of the trial experiment instrument of the new electrostatic generator

The charge recovery electrode (C) was partly bent as shown in figure 13 at the center. As a result, this hollow of the charge recovery electrode (C) can perform an Faraday gauge function. When the charge carrier (D) touch the back surface of the charge recovery electrode (C_2), almost all charge on the charge carrier (D) is transferred to the charge recovery electrode (C).

Figure 14 shows the charge recovery rate as a function of the depth of the hollow of the recovery electrode (C). This is a simulated result. It is desirable that the charge recovery rate is higher than 90%. Therefore, the depth was decided to be 30mm.
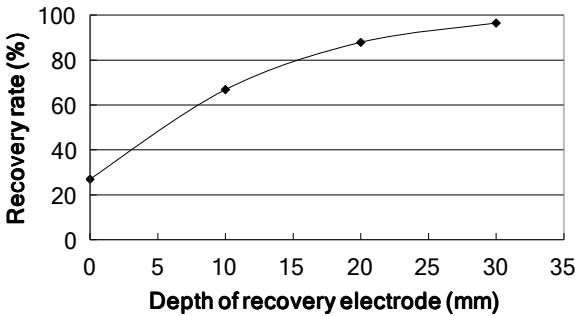

Fig. 14. The charge recovery rate as a function of the depth of the hollow of the recovery electrode.

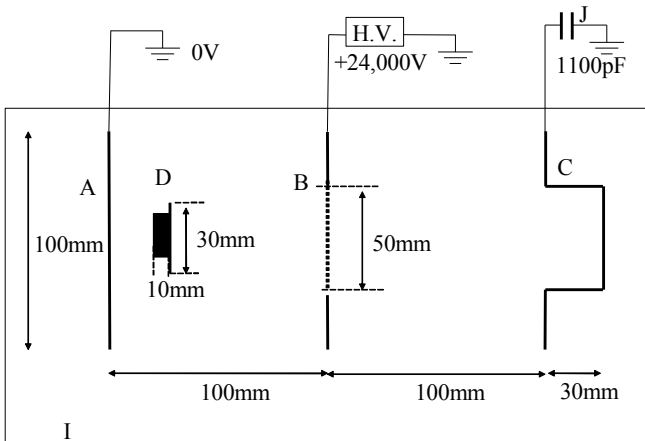Figure 15 shows the electric circuit of the trial experiment instrument.

Fig. 15. The Electric circuit of the trial experiment instrument of the new electrostatic generator

The three electrode (A,B,C) and the charge carrier (D) are electrically separated by the air and the insulating base plate (I) as shown in figure 15. The high voltage electrode (B) is applied +24,000V, and the charge injection electrode (A) and the charge recovery

electrode (C) are grounded. As a result, an electric field +0.24kV/mm is produced between the high voltage electrode (B) and the charge injection electrode (A). This electric field acts on negative charges on the charge carrier (D) and generate an electric force that force the charge carrier to the right. On the contrary, an electric field -0.24kV/mm is produced between the high voltage electrode (B) and the charge recovery electrode (C). This electric field acts on negative charges on the charge carrier (D) and generate an electric force that force the charge carrier to the left. As mentioned before, the former electrostatic force is larger than the latter electrostatic force. Because, the shape of the charge carrier (D) is asymmetric.

When the charge carrier (D) is set on the catapult (F) and touched to the charge injection electrode (A), some negative charge is injected to the charge carrier (D) from the charge injection electrode (A). This charge is transferred to the charge recovery electrode (C), and it is saved in the capacitor (J). The capacitance of the capacitor (J) is 1100pF, therefore potential of the capacitor (J) is risen when the charge is saved in the capacitor. This potential change can be measured by a surface potential meter.

III. EXPERIMENTAL RESULTS OF THE TRIAL INSTRUMENT

It is expected that the asymmetric charge carrier (D) is released from the catapult (F), passes through the high voltage electrodes (B) and hits the back surface of the recovery electrode (C_2). In this moving, the charge carrier (D) gets some charge from the injection electrode (A) and transports this charge to the recovery electrode (C). Then almost all charge is recovered by the recovery electrode (C). After that, the charge carrier (D) will return to the injection electrode (A) automatically.

Those steps must be confirmed one by one. Then, firstly the arrival positions of the charge carrier (D) to the front surface of the recovery electrode (C_1) were measured under no-electric field with using movie camera (Sony Cyber-shot DSC-P2) and the scale (K). This measurements were repeated 10 times. Figure 16 shows the arrival positions of the charge carrier (D) under no-electric field.
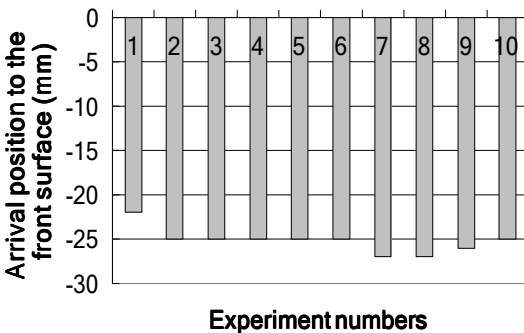

Fig. 16. The arrival positions of the charge carrier to the front surface of the recovery electrode under no-electric field.

The average arrival position of the charge carrier (D) to the front surface of the recovery electrode (C_1) under no-electric field was calculated as -25.2 mm from figure 16. If this experimental instrument is placed in a vacuum condition, the released charge carrier will reach to the front surface of the recovery electrode (C_1). Because the distance between the injection electrode (A) and the high voltage electrode (B) (100mm) is the same the distance between the high voltage electrode (B) and the front surface of the recovery electrode (C_1) (100mm).

However, the arrival position was 25.2mm short to the surface of the recovery electrode (C_1) in the air. Because there was an strong air resistance to this high speed moving charge carrier. Nevertheless, the asymmetric shape charge carrier can get some extra kinetic energy from electric field as described before. Therefore, the extra energy was expected to be able to transport the charge carrier from this arrival position to the back surface of the recovery electrode (C2). This distance is 55.2mm (25.2mm+30mm).

Then, the same experiment was performed under high electric field. In this experiment, +24kV was applied to the high voltage electrode (B). Figure 17 shows the arrival positions of the charge carrier (D) to the back surface of the recovery electrode (C_2) under high electric field.
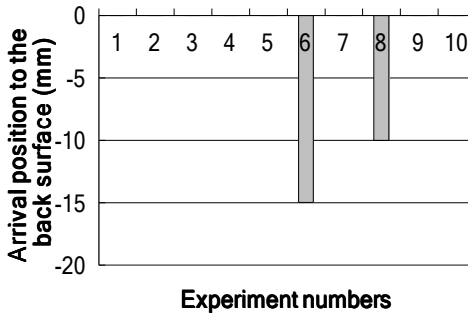

Fig. 17. The arrival positions of the charge carrier to the back surface of the recovery electrode under high electric field.

On eight experiments of the ten experiments, the charge carrier inclined about 90 degree as shown in figure 18.
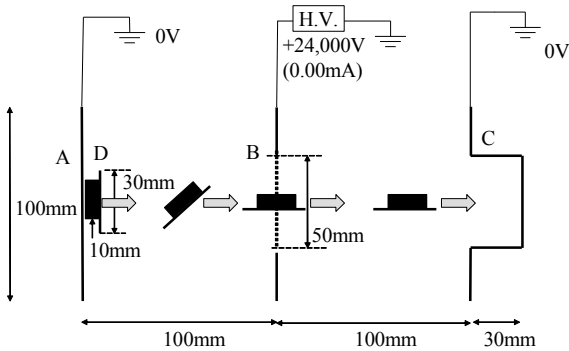
Fig. 18. Schematic explanation of the inclined charge carrier under high electric field.

The electrostatic force that acts on this inclined charge carrier (D) becomes weak. Therefore, those results were omitted. On the other two experiments, the charge carrier (D) moved with a little incline. Therefore. Those results were recognized as correct.

(By the way, it was observed that the charge carrier strongly hit on the back surface of the recovery electrode (C_2) in other experiment. However, this was not correct because the charge carrier had positive charge. Those positive charges were given to the charge carrier from the positive high voltage electrode by injection or corona diskharge. If the charge carrier kept negative charge, it must softly hit on the back surface of the recovery electrode (C2), or it must return without hitting as shown in this experiment movie.)

The average arrival position of the charge carrier (D) to the back surface of the recovery electrode (C_2) under high electric field was calculated as -12.5 mm from those results. The distance from the injection electrode (A) to this arrival position is 217.5mm. On the contrary, the distance from the injection electrode (A) to the back surface of the recovery electrode (C_2) is 230.0mm. Therefore, when the recovery electrode (C) is shifted to 12.5mm to left, the charge carrier (D) can hit the back surface of the recovery electrode (C_2) .

However the distance between the back surface of the recovery electrode (C_2) and the high voltage electrode (B) is reduced from 130mm to 117.5mm by this shift of the recovery electrode (C). The charge carrier (D) has to return from the back surface of the recovery electrode (C_2) to the injection electrode (A) automatically. Because there was no electrostatic force on the return course.

Then secondly, the returning positions of the charge carrier (D) to the injection electrode (A) were measured as a function of the distance between the back surface of the recovery electrode (C_2) and the high voltage electrode (B). This time the other catapult (F) was made on the back surface of the recovery electrode (C_2). Figure 19 shows the results.
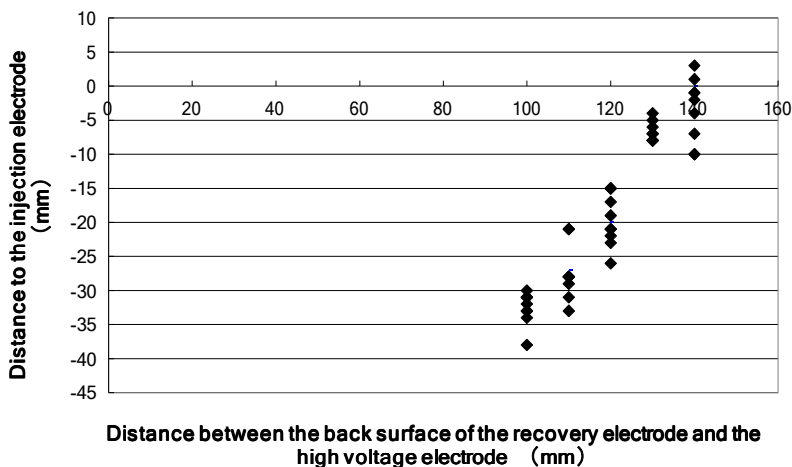
Fig. 19. The returning positions of the charge carrier to the injection electrode as a function of the distamce between the back surface of the recovery electrode and the high voltage electrode.

It is apparent from figure 19 that the distance between the back surface of the recovery electrode (C_2) and the high voltage electrode (B) needs 140 mm or over for the automatic return of the charge carrier (D). This result means that the extra energy has to transport the charge carrier 65.2mm or over. Nevertheless, the extra energy could transport the charge carrier only 42.7mm. The shortage was 22.5mm or over. This shortage will be reduced a little using higher voltage. But, higher voltage will produce a corona diskharge anyway.

As a result, it is very difficult for the charge carrier (D) to hit the back surface of the recovery electrode (C2) by this instrument. Therefore, it is not expected that this first trial instrument of the new electrostatic generator generate an electricity.

However, if the second trial instrument would be placed in vaccum condition, then this problem will be perfectly solved. Because, the extra energy can transport the charge carrier 42.7mm. On the contrary the required transportation distance is only 30mm with this vacuum instrument. The difference energy (12.7mm) will be converted into an electric energy.

IV. CONCLUSION

The first trial instrument of the new electrostatic generator unfortunately failed to generate an electricity. The main reason of the failure is that the air resistance to the charge carrier was stronger than the electrostatic force to the charge carrier. However this problem will be easily solved in the next trial instrument with a vacuum experimental box.

Furthermore this first trial instrument has another problem. The charge carrier moved with large incline under high electric field many times. The charge carrier has to move with no-incline any time. It is expected that this problem will be solved by the new design of the electrodes and the charge carrier.

As a result, the second trial instrument of the new electrostatic generator will generate an electricity next year, and the complete device of the new electrostatic generator will solve the CO_2 problem in the near future.

REFERENCES

[1]   David Halliday, Robert Resnick, Jearl Walker, Fundamentals of Physics. 6th edition   Japanese version Chapter "Electric Charge" question 1, Wiley & sons. Inc.
[2]   K. Sakai, et al., Electrostatics: Theory and Applications, first ed. Nova Science Publish, New York, 2010 (Chapter 1)
[3]   K. Sakai, Asymmetric Electrostatic Forces and a New Electrostatic Generator, first ed. Nova Science Publish, New York, 2010
[4]   K. Sakai, "The electrostatic force that acts on the charged asymmetric conductor in a high electric field," Proceedings of 2009 Electrostatics Joint Conference (2009) P2.07
[5]   K. Sakai, "Electrostatic force that acts on non-sphere shape charged conductors", Proceedings of 2010 ESA annual Conference (2010) G4
[6]   K. Sakai, "A simple experiment result that confirmed asymmetric electrostatic force", Proceedings of 2011 ESA annual Conference (2011) B4
[7]   K. Sakai, "Asymmetric electrostatic force", This is now contributed to Journal of Electrostatics.
[8]   K. Sakai, "What is the energy of an electric field?", Proceedings of 2012 ESA annual Conference (2012) PS13
[9]   Handbook of electrostatic, Japan, (1998) pp. 962
[10] Yasuyuki Matsubara, Improved Finite Difference Expression for Laplace's and Poisson's Equations on the Surface of Dielectrics, J. Electrostatics Japan 16 (1992) pp. 440-442
[11] Yasuyuki Matsubara, A Guide to the Calculation of Electric Field Part Ⅲ Application of the Finite Difference Method to Electric field in an Oil Tank, J. Electrostatics Japan 16 (1992) pp. 530-538
[12] Yasuyuki Matsubara, A Method to Calculate the Potential of Ungrounded Conductors, Proceedings of the Institute of Electrostatics Japan (1994) pp. 181-184
[13] T. Tsutsumino, Y. Suzuki, N. Kasagi, Y. Sakane, Seismic power generator using high-performance polymer electret, Proc. Int. Conf. MEMS'06, Jun. 2006, Istanbul, pp.98-101.